

Vector meson's spin alignments in high energy reactions

Jin-Hui Chen,^{1,*} Zuo-Tang Liang,^{2,†} Yu-Gang Ma,^{1,‡} Xin-Li Sheng,^{3,§} and Qun Wang^{4,5,¶}

¹*Key Laboratory of Nuclear Physics and Ion-beam Application (MoE),
Institute of Modern Physics, Fudan University, Shanghai 200433, China*

²*Institute of Frontier and Interdisciplinary Science,
Key Laboratory of Particle Physics and Particle Irradiation (MOE),
Shandong University, Qingdao, Shandong 266237, China*

³*INFN-Firenze, Via Giovanni Sansone, 1, 50019 Sesto Fiorentino FI, Italy*

⁴*Department of Modern Physics, University of Science and Technology of China, Hefei, Anhui 230026, China*

⁵*School of Mechanics and Physics, Anhui University of Science and Technology, Huainan, Anhui 232001, China*

The global spin alignment of vector mesons has been observed by the STAR collaboration at the Relativistic Heavy Ion Collider (RHIC) at Brookhaven National Laboratory (BNL). It provides a unique opportunity to probe the correlation between the polarized quark and antiquark in the strongly coupled quark-gluon plasma (sQGP) produced in relativistic heavy ion collisions, opening a new window to explore the properties of sQGP. In addition, spin alignments of vector mesons have also been observed in other high-energy particle collisions. The results seem to be strongly dependent on the hadronization mechanism, so comprehensive studies are needed. In this article, we present a brief review of theoretical and experimental advances in the study of vector meson's spin alignments in a variety of high-energy particle collisions, with emphasis on hadronization mechanisms.

I. INTRODUCTION

Quantum Chromodynamics (QCD) is the fundamental theory for strong interaction that is responsible for binding quarks and gluons together to form protons, neutrons, and other hadrons. Relativistic Heavy Ion Collisions (RHIC) are a powerful tool for studying Quantum Chromodynamics (QCD) and properties of strongly interacting matter under extreme conditions [1–6]. In these collisions, heavy nuclei are accelerated to nearly light speed and then collide to achieve immense energy density that recreates conditions similar to those just microseconds after the Big Bang, allowing scientists to study quark-gluon plasma (QGP) - a state of matter in which quarks and gluons are decoupled from hadrons [7–13].

Spin is an intrinsic form of angular momentum carried by elementary particles, and it is a (pseudo-)vector quantity that can point to different directions. As elementary particles of strong interaction, quarks and gluons carry spins. As composite particles of strong interaction, many hadrons also carry spins. The spin polarization refers to the alignment of the spin along a specific direction (called spin quantization direction). Spin degrees of freedom have been playing an important role in the development of modern physics since its discovery in 1925. The global polarization effect (GPE) of the quark gluon plasma (QGP) produced in high energy heavy-ion collisions is a new spin effect in particle and nuclear physics. The theoretical prediction [14, 15] was made

almost two decades ago and attracted immediate attention [16–25]. However the enthusiasm was soon dampened by STAR's earlier attempts [21, 23–25] that gave null results for global Λ -hyperon polarization as well as global spin alignments of vector mesons due to limited statistics in data at that time. The earlier results show that the GPE, even if it exists, could be very small, so it is unclear if it is within the scope and resolution of current experiments. The enthusiasm was aroused by non-vanishing results for the GPE for Λ hyperons in STAR's beam-energy-scan experiments [26], which showed that the GPE decreases monotonically with collision energies. Now the GPE has grown to be a sub-field in heavy-ion collisions, see Refs. [27–34] for recent reviews.

Another surprise came five years later from STAR's measurements on the global spin alignment of ϕ mesons with high statistics [35]. The STAR's results [35] seem to conflict with hyperon's polarization as predicted in Ref. [15] that the vector meson's spin alignment is proportional to quark polarization squared and thus should be much smaller than that observed in STAR's experiment [35]. So STAR's results are definitely non-trivial and may have deep implication for hadronization mechanism and properties of QCD [36–39]. When a system of particles exhibits spin polarization, it means that the spins of these particles are aligned more often in a particular direction than randomly oriented. Now the global spin alignment of vector mesons has attracted a broad interest in experimental and theoretical communities [40–45]. Spin polarization in the context of QCD is a critical aspect of understanding the internal structure and dynamics of hadrons. Through both theoretical and experimental approaches, physicists aim to unravel the complexities of how quarks and gluons contribute to the spin and other properties of hadrons. Several theoretical interpretations have been proposed and new measurements are underway.

* chenjinhui@fudan.edu.cn

† liang@sdu.edu.cn

‡ mayugang@fudan.edu.cn

§ sheng@fi.infn.it

¶ qunwang@ustc.edu.cn

In addition to relativistic heavy-ion collisions, the vector meson's spin alignment has also been studied in other high energy processes such as e^+e^- , e^-p and pp collisions [46–50]. The results show quite different features and theoretical efforts have also been made to describe them [51–58]. It is therefore desirable to summarize these experimental and theoretical results and make comparison among different high energy reactions as guidance for future studies.

Firstly, we briefly review spin density matrices for vector mesons as well as measurement methods for the spin alignment, and then review experimental results in different high energy collisions. Secondly, we summarize theoretical approaches in two different hadronization mechanisms as well as the linear response theory for the spin alignment of vector mesons in thermalized QGP. Finally, we present a short summary and outlook.

II. SPIN DENSITY MATRICES AND MEASUREMENT METHODS FOR SPIN ALIGNMENT

A. Spin density matrices

The spin polarization of particles produced in high energy reaction can be described by the spin density matrix $\hat{\rho}$. For particles with spin-1/2 such as quarks and antiquarks, $\hat{\rho}_q$ is a 2×2 Hermitian matrix which can be expanded as

$$\hat{\rho}_q = \frac{1}{2}(1 + \vec{P}_q \cdot \vec{\sigma}), \quad (1)$$

where $\vec{\sigma} = (\sigma_x, \sigma_y, \sigma_z)$ are Pauli matrices, and $\vec{P}_q = \text{Tr}(\vec{\sigma}\hat{\rho}_q)$ is the mean spin polarization vector in the quark's rest frame.

For spin-1 particles, the spin density matrix is a 3×3 Hermitian matrix. With the spin quantization axis specified, the spin states are denoted as $|jm\rangle$ and the spin density matrix can be put into the form [59]

$$\begin{aligned} \hat{\rho}_V &= \begin{pmatrix} \rho_{11} & \rho_{10} & \rho_{1-1} \\ \rho_{01} & \rho_{00} & \rho_{0-1} \\ \rho_{-11} & \rho_{-10} & \rho_{-1-1} \end{pmatrix} \\ &= \frac{1}{3} + \frac{1}{2}P_i\Sigma_i + T_{ij}\Sigma_{ij}, \end{aligned} \quad (2)$$

where $i, j=1,2,3$, and Σ_i and Σ_{ij} are 3×3 traceless matrices defined as [34, 42]

$$\begin{aligned} \Sigma_1 &= \frac{1}{\sqrt{2}} \begin{pmatrix} 0 & 1 & 0 \\ 1 & 0 & 1 \\ 0 & 1 & 0 \end{pmatrix}, \\ \Sigma_2 &= \frac{1}{\sqrt{2}} \begin{pmatrix} 0 & -i & 0 \\ i & 0 & -i \\ 0 & i & 0 \end{pmatrix}, \end{aligned}$$

$$\begin{aligned} \Sigma_3 &= \begin{pmatrix} 1 & 0 & 0 \\ 0 & 0 & 0 \\ 0 & 0 & -1 \end{pmatrix}, \\ \Sigma_{ij} &= \frac{1}{2}(\Sigma_i\Sigma_j + \Sigma_j\Sigma_i) - \frac{2}{3}\delta_{ij}. \end{aligned} \quad (3)$$

The polarization vector $\vec{\varepsilon}_m$ in the rest frame of the spin-1 particle in the spin state $|1m\rangle$ can be defined as

$$\vec{\varepsilon}_{m=0} = \hat{z}, \quad (4)$$

$$\vec{\varepsilon}_{m=\pm 1} = \mp \frac{1}{\sqrt{2}}(\hat{x} \pm i\hat{y}), \quad (5)$$

where the spin quantization direction is assumed to be \hat{z} direction.

The spin vector \vec{S} is related to the polarization vector $\vec{\varepsilon}$ by $\vec{S} = \text{Im}(\vec{\varepsilon}_m^* \times \vec{\varepsilon}_m)$. If the vector meson is in the pure spin state with $m=0$, the spin vector is vanishing, $\vec{S} = \vec{\varepsilon}_0 \times \vec{\varepsilon}_0 = 0$. If the vector meson is in the pure spin state with $m=\pm 1$ we have $\vec{S} = \text{Im}(\vec{\varepsilon}_{\pm 1}^* \times \vec{\varepsilon}_{\pm 1}) = \pm \hat{z}$, which is parallel or anti-parallel to the spin quantization direction.

B. Measurement of spin density matrix through angular distribution of decay product

In high energy reactions, the spin polarization of a particle A is mainly measured through the angular distribution of its decay product in two-body decay $A \rightarrow 1 + 2$ in the rest frame of A . The corresponding formulae are derived using symmetry properties and conservation laws in the decay process.

In the rest frame of A , the momenta of the particle 1 and 2 are denoted as $\vec{p} = \vec{p}_1 = -\vec{p}_2$, and their spin states are labeled by their helicities λ_1 and λ_2 respectively. The decay amplitude is given by,

$$A_m(\vec{p}; \lambda_1 \lambda_2) = \langle \vec{p}; \lambda_1 \lambda_2 | \hat{U} | j_A m_A \rangle, \quad (6)$$

where \hat{U} stands for the transition operator, $|j_A m_A\rangle$ denotes the spin state of A , and $|\vec{p}; \lambda_1 \lambda_2\rangle$ is the helicity state of decay daughters.

We can insert the completeness identity for the helicity states of the two-particle system $|E; jm; \lambda_1 \lambda_2\rangle$ with fixed E (the energy of the system), j (total angular momentum quantum number) and m (the eigenvalue of j_z). From energy and angular momentum conservation laws in the decay process in A 's rest frame, we have $E = M_A$ (the mass of A), $j = j_A$ and $m = m_A$. So we obtain,

$$\begin{aligned} A_m(\vec{p}; \lambda_1 \lambda_2) &= \langle \vec{p}; \lambda_1 \lambda_2 | M_A; j_A m_A; \lambda_1 \lambda_2 \rangle \\ &\quad \times \langle M_A; j_A m_A; \lambda_1 \lambda_2 | \hat{U} | j_A m_A \rangle. \end{aligned} \quad (7)$$

The space rotation invariance demands that the helicity amplitude

$$\langle M_A; j_A m_A; \lambda_1 \lambda_2 | \hat{U} | j_A m_A \rangle \equiv H_A(\lambda_1, \lambda_2), \quad (8)$$

is independent of m_A . So we obtain,

$$A_m(\vec{p}; \lambda_1 \lambda_2) = \langle \vec{p}; \lambda_1 \lambda_2 | M_A; j_A m_A; \lambda_1 \lambda_2 \rangle H_A(\lambda_1, \lambda_2). \quad (9)$$

We see that the angular dependence is solely given by the inner product $\langle \vec{p}; \lambda_1 \lambda_2 | M_A; j_A m_A; \lambda_1 \lambda_2 \rangle$, which we calculate as follows. First, we calculate it for \vec{p} in z -direction, i.e., $\langle p, 0, 0; \lambda_1 \lambda_2 | M_A; j_A m_A; \lambda_1 \lambda_2 \rangle$, which gives a constant $\sqrt{(2j_A + 1)/4\pi}$ independent of m_A . We then transform $|p, 0, 0; \lambda_1 \lambda_2\rangle$ to $|p, \theta, \varphi; \lambda_1 \lambda_2\rangle$ in the direction of \vec{p} by a spatial rotation. The rotation can be achieved by three successive rotations in Euler angles $(\alpha, \beta, \gamma) = (\varphi, \theta, -\varphi)$ that rotate $\vec{p} = (p, 0, 0)$ to $\vec{p} = (p, \theta, \varphi)$ with the rotation operator [60]

$$\hat{R}(\varphi, \theta, -\varphi) = e^{-i\varphi \hat{J}_z} e^{-i\theta \hat{J}_y} e^{i\varphi \hat{J}_z}. \quad (10)$$

Hence, we obtain the inner product as

$$\begin{aligned} & \langle \vec{p}; \lambda_1 \lambda_2 | M_A; j_A m_A; \lambda_1 \lambda_2 \rangle \\ &= \sqrt{\frac{2j_A + 1}{4\pi}} d_{m_A \lambda}^{j_A*}(\theta) e^{i(m_A - \lambda)\varphi}, \end{aligned} \quad (11)$$

where $d_{mm'}^j(\theta) = \langle jm | e^{-i\theta \hat{J}_y} | jm' \rangle$ is the element of the Wigner rotation matrix and $\lambda = \lambda_1 - \lambda_2$. We note that the definition of the rotation operator \hat{R} in (10) introduces an additional rotation $\gamma = -\varphi$ relative to that in Ref. [61].

The spin density matrix of the system of particles 1 and 2 can be defined as

$$\hat{\rho}_{12} = \hat{U} \hat{\rho}^A \hat{U}^\dagger, \quad (12)$$

where ρ^A is the spin density matrix of A. Then the angular distribution is given by

$$\begin{aligned} W(\theta, \varphi) &= N \sum_{\lambda_1, \lambda_2} \langle \vec{p}; \lambda_1, \lambda_2 | \hat{\rho}_{12} | \vec{p}; \lambda_1, \lambda_2 \rangle \\ &= N \sum_{\lambda_1, \lambda_2; m_A, m'_A} |H_A(\lambda_1, \lambda_2)|^2 \rho_{m_A m'_A}^A \\ &\quad \times e^{i(m_A - m'_A)\varphi} d_{m_A \lambda}^{j_A*}(\theta) d_{m'_A \lambda}^{j_A}(\theta), \end{aligned} \quad (13)$$

where $\rho_{m_A m'_A}^A = \langle m_A | \hat{\rho}^A | m'_A \rangle$ denotes elements of $\hat{\rho}^A$.

Since the helicity amplitude $H_A(\lambda_1, \lambda_2)$ is generally unknown, only in some special cases one can use $W(\theta, \varphi)$ to determine elements of $\hat{\rho}^A$. Here are three such cases.

(1) $j_A = 1/2$, $\lambda_1 = \pm 1/2$, $\lambda_2 = 0$, as in a spin-1/2 baryon's decay into a spin-1/2 baryon and a pion, $H \rightarrow B\pi$. In this case, we have two independent helicity amplitudes $H_A(\pm 1/2, 0)$ and $W(\theta, \varphi)$ is given by

$$W(\theta, \varphi) = \frac{1}{4\pi} \left(1 + \alpha_A \vec{P}_A \cdot \vec{n} \right), \quad (14)$$

where $\vec{P}_A = \text{Tr}(\vec{\sigma} \hat{\rho}_A)$ is the polarization vector of A, $\vec{n} = \vec{p}/|\vec{p}|$ is the momentum direction and

$$\alpha_A = \frac{H_A(1/2, 0) - H_A(-1/2, 0)}{H_A(1/2, 0) + H_A(-1/2, 0)}, \quad (15)$$

is the decay parameter for $A \rightarrow 1 + 2$. We also see that if parity is conserved in the decay process so that $H_A(1/2, 0) = H_A(-1/2, 0)$, we then have $\alpha_A = 0$ and the isotropic distribution $W(\theta, \varphi) = 1/4\pi$. So Eq. (14) can be used to determine \vec{P}_A only in weak decays.

(2) $j_A = 1$, $\lambda_1 = \lambda_2 = 0$, such as in the vector meson's decay into two pions, $V \rightarrow \pi\pi$. In this case, the helicity amplitude $H_A(0, 0)$ is a trivial constant that can be absorbed into the normalization constant, so that

$$\begin{aligned} W(\theta, \varphi) &= \frac{3}{8\pi} \left\{ (1 - \rho_{00}^A) + (3\rho_{00}^A - 1) \cos^2 \theta \right. \\ &\quad - 2 \sin^2 \theta [\cos 2\varphi \text{Re} \rho_{1-1}^A - \sin 2\varphi \text{Im} \rho_{1-1}^A] \\ &\quad - \sqrt{2} \sin 2\theta [\cos \varphi (\text{Re} \rho_{10}^A - \text{Re} \rho_{-10}^A) \\ &\quad \left. - \sin \varphi (\text{Im} \rho_{10}^A + \text{Im} \rho_{-10}^A)] \right\}, \end{aligned} \quad (16)$$

If we integrate over φ , we obtain,

$$W(\theta) = \frac{3}{4} \left\{ (1 - \rho_{00}^A) + (3\rho_{00}^A - 1) \cos^2 \theta \right\}. \quad (17)$$

We see that by measuring the distribution in θ one can extract the value of ρ_{00}^A .

(3) $j_A = 1$, $\lambda_1 = \pm 1/2$, $\lambda_2 = \pm 1/2$, such as in the vector meson's decay into a dilepton pair, $V \rightarrow e^+ e^-$. Here, we have four combinations of λ_1 and λ_2 . In this case, only if parity and helicity conservation are valid so that $H_A(-\lambda_1, -\lambda_2) = H_A(\lambda_1, \lambda_2)$ and $H_A(\lambda_1, \lambda_2) \neq 0$ only for $\lambda_1 = -\lambda_2$, only one non-vanishing helicity amplitude is left and can be absorbed into the normalization constant. We then obtain the angular distribution as

$$\begin{aligned} W(\theta, \varphi) &= \frac{3}{8\pi(1 + \rho_{00}^A)} \left\{ 1 + \lambda_\theta \cos^2 \theta \right. \\ &\quad + \lambda_\varphi \sin^2 \theta \cos 2\varphi + \lambda_{\theta\varphi} \sin 2\theta \sin 2\varphi \\ &\quad \left. + \lambda_\varphi^\perp \sin^2 \theta \sin 2\varphi + \lambda_{\theta\varphi}^\perp \sin 2\theta \sin \varphi \right\}, \end{aligned} \quad (18)$$

where the λ coefficients are related to elements of ρ^A by

$$\lambda_\theta = \frac{1 - 3\rho_{00}^A}{1 + \rho_{00}^A}, \quad (19)$$

$$\lambda_\varphi = \frac{2\text{Re} \rho_{1-1}^A}{1 + \rho_{00}^A}, \quad (20)$$

$$\lambda_{\theta\varphi} = \frac{\sqrt{2}\text{Re}(\rho_{10}^A - \rho_{-10}^A)}{1 + \rho_{00}^A}, \quad (21)$$

$$\lambda_\varphi^\perp = -\frac{2\text{Im} \rho_{1-1}^A}{1 + \rho_{00}^A}, \quad (22)$$

$$\lambda_{\theta\varphi}^\perp = -\frac{\sqrt{2}\text{Im}(\rho_{10}^A + \rho_{-10}^A)}{1 + \rho_{00}^A}. \quad (23)$$

In principle, one can extract elements of ρ^A from $W(\theta, \varphi)$ through these coefficients.

Measurements on hyperon polarization and vector meson's spin alignment have been carried out in different

high energy reactions using Eqs. (14-18) (see e.g. Refs. [62–68], [46–50] and [21, 23–25]). In this brief review, we concentrate on spin alignment of vector mesons with light flavors in comparison with hyperon polarization, thus only Eqs. (14) and (16) are involved.

III. EXPERIMENTAL RESULTS

A. Vector meson’s spin alignments in e^+e^- -annihilations

The earliest measurements of vector meson’s spin alignments in high energy reactions might be made at the Large Electron-Positron collider (LEP) at European Organization for Nuclear Research (CERN) in the 1990s [46–49], where one of the popular polarization axis was the helicity axis defined by the individual particle’s momentum direction. Measurements have been carried out by DELPHI and OPAL Collaborations for K^{*0} and ϕ mesons and even for heavy flavor meson such B and D^* [46–49]. They also measured the off-diagonal element such as $\rho_{1,-1}$. As an example, we show the results from Ref. [47] in Fig. 1.

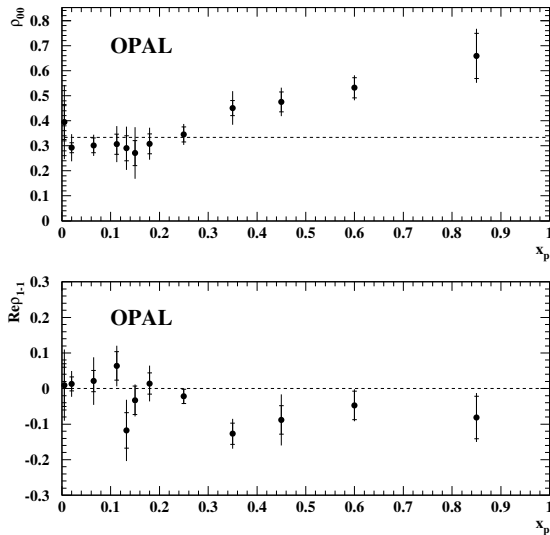


FIG. 1. Experimental data obtained by OPAL Collaboration at LEP for the spin alignment ρ_{00} and off-diagonal element $\rho_{1,-1}$ of K^{*0} . This figure is taken from Ref.[47].

From these measurements [46–49] in e^+e^- collisions, we see clearly that ρ_{00} is significantly larger than $1/3$ in the fragmentation region $x_p > 0.3$ ($x_p \equiv p/p_{\text{beam}}$) which show that the spin of vector mesons is significantly aligned in that region. However, at small fractional momenta $x_p \leq 0.3$, null results for K^{*0} and ϕ mesons were reported in e^+e^- collisions [46, 47].

The data have attracted much theoretical attention [51–58] and we will come back to this later in Sec. VI.

B. Global spin alignments of vector mesons in heavy-ion collisions

Measurements of the vector meson’s spin alignment in heavy-ion collisions are different from conventional studies. A new polarization axis along the nucleus-nucleus system’s orbital angular momentum can be defined [14, 15].

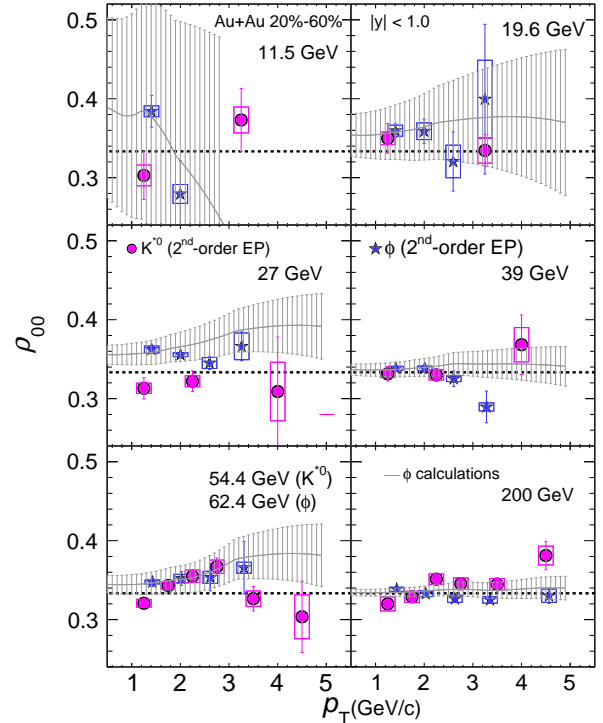


FIG. 2. Measurements of the vector meson’s spin density matrix element ρ_{00} as functions of transverse momentum (p_T) for K^{*0} and ϕ mesons in Au+Au collisions at different energies. Data points are STAR’s measurements [35], bands are theoretical calculations for ϕ mesons [39].

In 2008 the STAR Collaboration performed a measurement of the vector meson’s global spin alignment in Au+Au collisions at $\sqrt{s_{NN}} = 200$ GeV. Due to limited statistics and only covered top RHIC collision energies, no significant results were reported [24]. Since 2010, the collaboration has been collecting and analyzing data of higher statistics and at lower collision energies, including data in the Beam Energy Scan Phase I (BES-I) runs and high statistics Au+Au runs at $\sqrt{s_{NN}} = 200$ GeV. The analysis was focused on mid-central collisions (20-60%) where larger system angular momenta are expected in comparison with the values in central or peripheral collisions. Fig. 2 presents the transverse momentum dependence of ρ_{00} for K^{*0} and ϕ in 20-60% central Au+Au

collisions at $\sqrt{s_{NN}} = 11.5, 19.6, 27, 39, 62.4$ (54.4), 200 GeV. The ρ_{00} results show a non-trivial p_T dependence. For K^{*0} mesons at $\sqrt{s_{NN}} = 54.4$ and 200 GeV, they are larger than $1/3$ with about 2σ significance at intermediate p_T . At low beam energies the statistics is not sufficient to observe any significant deviation from $1/3$. From the calculation in Ref. [15], one naively expect ρ_{00} to be smaller than $1/3$ due to hadronization of the polarized quark and antiquark via quark combination, and larger than $1/3$ due to fragmentation of the quark and antiquark. On the other hand, for ϕ mesons for all energies considered, we see that the departure of ρ_{00} from $1/3$ mainly occurs at $p_T \sim 1.0 - 2.4$ GeV/c, while at higher p_T the result can be regarded as being consistent with $1/3$ within $\sim 2\sigma$ or less significance.

The STAR collaboration also studied the collision energy dependence by integrating $\rho_{00}(p_T)$ with the weight $1/(\text{stat. error})^2$. Fig. 3 presents ρ_{00} for K^{*0} and ϕ mesons in 20-60% central Au+Au collisions at collision energies ranging from $\sqrt{s_{NN}} = 11.5$ to 200 GeV [35]. We see that ρ_{00} for ϕ mesons increases with decreasing the collision energy, while ρ_{00} for K^{*0} mesons fluctuates around $1/3$ with the collision energy. To quantify the effect, the average of ρ_{00} is taken over lower collision energies for K^{*0} and ϕ . The ρ_{00} for ϕ mesons, averaged over beam energies between 11.5 and 62.4 GeV, is 0.3512 ± 0.0017 (stat.) ± 0.0017 (syst.). Taking the total uncertainties as the sum in quadrature of statistical and systematic uncertainties, the result indicates that ρ_{00} for ϕ mesons is above $1/3$ with a significance of 7.4σ , representing the first observation of the global spin alignment. The ρ_{00} for K^{*0} mesons, averaged over beam energies between 11.5 and 54.4 GeV, is 0.3356 ± 0.0034 (stat.) ± 0.0043 (syst.) and is consistent with $1/3$. The measurements of the ALICE collaboration in Pb+Pb collisions at 2.76 TeV [69], taken from the closest data points to the mean p_T for the p_T range used in STAR's measurements, are also shown for comparison in Fig. 3. The ρ_{00} data point for K^{*0} and ϕ mesons from ALICE collaboration is more or less consistent with $1/3$ with large uncertainties.

According to various studies, there are many sources that contribute to the global spin alignment of ϕ mesons including vortical flows [36], electromagnetic fields [36] generated by the electric currents carried by the colliding nuclei, local spin alignment [71], quark polarization along the direction of its momentum (helicity polarization) [72], the spin alignment by fragmentation [15] of polarized quarks, and the shear stress tensor [73–75]. However, these conventional mechanisms are not sufficient to account for the observed ρ_{00} for ϕ mesons. It was also proposed that local correlations or fluctuations in turbulent color fields [76] and glasma fields [77] can also generate a significant contribution to ρ_{00} . A recent theoretical development based on local correlations or fluctuations of ϕ vector fields can describe the experimental data. The ϕ vector field is the '33' component of the SU(3) vector multiplet induced by currents of pseudo-Goldstone bosons [78], and it can polarize s and \bar{s} quarks in the

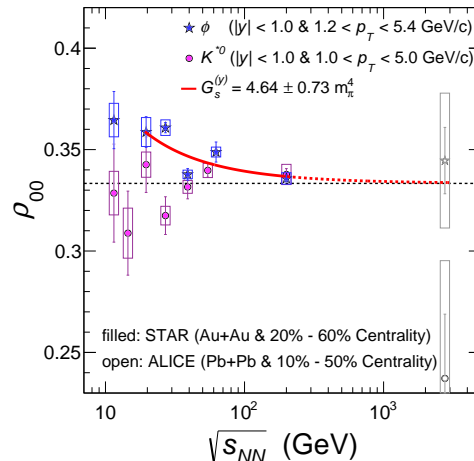


FIG. 3. Measurements of ρ_{00} with respect to the system orbital angular momentum in high energy heavy-ion collisions. Stars represent the data for ϕ mesons [35, 69], circles represent the data for K^{*0} mesons [35, 69]. The solid red line is the prediction from a non-relativistic coalescence model with strong force fields [37]. More sophisticated and complete calculations using the relativistic coalescence model and spin kinetic equation [38] were presented in Ref. [39, 70].

same way as the electromagnetic field does. The solid curve of Fig. 3 is such a fit to the data. We see that the calculation describes the data reasonably well. The correlation of the ϕ vector field can be quantified by $\langle \vec{E}_\phi^2 \rangle$ and $\langle \vec{B}_\phi^2 \rangle$ and can be extracted by fitting data, where \vec{E}_ϕ and \vec{B}_ϕ are electric and magnetic components of the ϕ vector field respectively. We will discuss more details about the theoretical model in Sect. IV B.

IV. VECTOR MESON'S SPIN ALIGNMENTS IN QUARK COMBINATION MODELS

It was well-known that huge angular momenta are generated in non-central high energy heavy-ion collisions [14, 22]. Due to spin-orbit couplings in QCD interaction, such huge angular momenta lead to the global polarization in quark scatterings in the form of the hyperon polarization [14, 22] and vector meson's spin alignment [15], the so-called GPE.

The GPE depends not only on the global quark polarization but also on the hadronization mechanism. In relativistic heavy-ion collisions, it is envisaged that a system of deconfined quarks and anti-quarks is created in the central rapidity and moderate transverse momentum region. Various aspects of experimental data suggest that hadronization of the system proceeds via combination of quarks and anti-quarks, a mechanism phrased as “quark recombination”, “quark coalescence” or simply as “quark combination”. We simply refer to it as “quark combina-

tion model” or “quark coalescence model” in this paper. We will summarize the results of vector meson’s spin alignments by the quark combination model in this section.

A. Vector meson’s spin alignments in non-relativistic quark combination models

In a non-relativistic quark combination model, the physics in the process that q (quark) and \bar{q} (antiquark) combine to M (meson) can be demonstrated in a clear way. Here, it is envisaged that in the combination process the vector meson’s spin is just the sum over the quark’s and anti-quark’s spins. Hence the spin density matrix and the spin alignment of the vector meson can be calculated from that of the quark and anti-quark. Such a calculation is straightforward and was carried out in Ref. [15], which we will summarize in this subsection.

The global quark polarization was taken as a constant so that the spin density matrix for the quark and anti-quark takes the diagonal form [15]

$$\hat{\rho}^q = \frac{1}{2} \begin{pmatrix} 1 + P_q & 0 \\ 0 & 1 - P_q \end{pmatrix}. \quad (24)$$

The spin density matrix of the $q_1\bar{q}_2$ system was taken as a direct product of the quark’s and anti-quark’s,

$$\hat{\rho}^{q_1\bar{q}_2} = \hat{\rho}^{q_1} \otimes \hat{\rho}^{\bar{q}_2}. \quad (25)$$

The elements of the spin density matrix $\hat{\rho}^V$ for the vector meson is obtained from $\hat{\rho}^{q_1\bar{q}_2}$ as

$$\rho_{m'm}^V = \langle jm' | \hat{\rho}^{q_1\bar{q}_2} | jm \rangle, \quad (26)$$

which leads to

$$\begin{aligned} \rho_{m'm}^V &= \sum_{m_1, m_2, m'_1, m'_2} \rho_{m'_1 m'_2, m_1 m_2}^{q_1 \bar{q}_2} \\ &\times \langle j_V m' | m'_1 m'_2 \rangle \langle m_1 m_2 | j_V m \rangle, \end{aligned} \quad (27)$$

where $|j_V m\rangle$ is the vector meson’s spin state in the constituent quark model with $j_V = 1$ and $m = 0, \pm 1$, and $\langle j_V m | m_1 m_2 \rangle$ are Clebsch-Gordan coefficients. After a straightforward calculation, we obtain the normalized spin alignment ρ_{00}^V as [15],

$$\rho_{00}^V = \frac{1 - P_{q_1} P_{\bar{q}_2}}{3 + P_{q_1} P_{\bar{q}_2}}. \quad (28)$$

If we take $P_{q_1} = P_{\bar{q}_2} = P_q$ (flavor blind for quarks and antiquarks), we simply obtain

$$\rho_{00}^V = \frac{1 - P_q^2}{3 + P_q^2}. \quad (29)$$

In exact the same way, we obtain the global hyperon polarization $P_H = P_q$ for Λ , Σ , and Ξ [14].

From Eqs. (28) and (29), we see that, in contrast to P_H , ρ_{00}^V is quadratic in P_q and should be less than 1/3. We emphasize that the case considered in Ref. [15] is over simplified in the fact that only the spin degree of freedom for the quark and antiquark is considered, neglecting other degree(s) of freedom and the correlation among the quark’s and antiquark’s polarization. So it might not be a surprise that the STAR data [26, 35] for the global spin alignment of ϕ mesons show a large deviation from 1/3, far beyond the value estimated from P_Λ ’s data by its square. In fact, if we make a step forward by considering the dependence of P_q on other degree of freedom [37–39, 79] $P_{q_1} P_{\bar{q}_2}$ in Eq. (28) should be replaced by $\langle P_{q_1} P_{\bar{q}_2} \rangle$, so we have

$$\rho_{00}^V = \frac{1 - \langle P_{q_1} P_{\bar{q}_2} \rangle}{3 + \langle P_{q_1} P_{\bar{q}_2} \rangle}. \quad (30)$$

The STAR data [26, 35] indicate

$$\langle P_{q_1} P_{\bar{q}_2} \rangle \neq \langle P_{q_1} \rangle \langle P_{\bar{q}_2} \rangle. \quad (31)$$

This means that there should be a strong correlation between the polarization of the quark and antiquark. Hence, the study of the global spin alignment for the vector meson in heavy-ion collisions provides a unique opportunity for exploring the local correlation in the quark’s and antiquark’s polarization, a new window for the study of properties of QGP.

It is also emphasized in Ref. [80] that the average in Eq. (30) is two-folded: the first average is taken inside the vector meson’s wave function (local correlation) and the second average is taken in the range outside the vector meson’s wave function (long-range correlation). More measurements are needed to tell the difference between two types of correlation [80]. A systematic formulation has been presented in [81]. It has been extended to spin 3/2 baryons in [82].

B. Vector meson’s spin alignments in quark combination models with phase space dependence

1. Non-relativistic model

In this subsection, we consider the non-relativistic quark combination model with phase space dependence [42, 79]. We extend the density operator (1) to the phase space as

$$\begin{aligned} \hat{\rho}^q &= \sum_{rs} \int [d^3 \vec{p}] [d^3 \vec{q}] \int d^3 \vec{x} e^{-i\vec{q} \cdot \vec{x}} \\ &\times w_{rs}^q(\vec{x}, \vec{p}) \left| r, \vec{p} + \frac{\vec{q}}{2} \right\rangle \left\langle s, \vec{p} - \frac{\vec{q}}{2} \right|, \end{aligned} \quad (32)$$

where $r, s = \pm$ denote spin states, $|r, \vec{p}\rangle$ denotes the spin-momentum state, and the momentum measure is defined as $[d^3 \vec{p}] \equiv d^3 \vec{p} / (2\pi)^3$. The weight function $w_{rs}^q(\vec{x}, \vec{p})$ is

the Wigner function in the spin-phase space and can be obtained as

$$w_{rs}^q(\vec{x}, \vec{p}) = \int [d^3\vec{q}] e^{i\vec{q}\cdot\vec{x}} \left\langle r, \vec{p} + \frac{\vec{q}}{2} \left| \hat{\rho}^q \right| s, \vec{p} - \frac{\vec{q}}{2} \right\rangle. \quad (33)$$

It is a 2×2 Hermitian matrix in the spin space and can be parameterized as

$$w_{rs}^q(\vec{x}, \vec{p}) = \frac{1}{2} f_q(\vec{x}, \vec{p}) \left[\delta_{rs} + \vec{\sigma}_{rs} \cdot \vec{P}_q(\vec{x}, \vec{p}) \right]. \quad (34)$$

Here $f_q(\vec{x}, \vec{p})$ is the un-polarized distribution function, and $\vec{P}_q(\vec{x}, \vec{p})$ is the spin polarization in phase space. The density operator for the anti-quark can be defined in the same way. The density operator for a quark-antiquark pair $q_1\bar{q}_2$ is defined from the direct product of quark's and anti-quark's one as $\hat{\rho}^{q_1\bar{q}_2} \equiv \hat{\rho}^{q_1} \otimes \hat{\rho}^{\bar{q}_2}$. The Wigner function can be normalized as

$$\sum_s \int d^3\vec{x} \int [d^3\vec{p}] w_{ss}(\vec{x}, \vec{p}) = 1. \quad (35)$$

The quark's spin quantization direction can be any direction, e.g., the z -direction, without loss of generality.

The elements of the vector meson's density matrix are obtained as

$$\begin{aligned} & \rho_{m'm}^V(\vec{x}, \vec{p}) \\ &= \frac{1}{N(\vec{x}, \vec{p})} \int [d^3\vec{q}] e^{i\vec{q}\cdot\vec{x}} \\ & \times \left\langle j_V m'; \vec{p} + \frac{\vec{q}}{2} \left| \hat{\rho}^{q_1} \otimes \hat{\rho}^{\bar{q}_2} \right| j_V m; \vec{p} - \frac{\vec{q}}{2} \right\rangle \\ &= \frac{1}{N(\vec{x}, \vec{p})} \int d^3\vec{x}_b [d^3\vec{p}_b] [d^3\vec{q}_b] \exp(-i\vec{q}_b \cdot \vec{x}_b) \\ & \times \varphi_V^* \left(\vec{p}_b + \frac{\vec{q}_b}{2} \right) \varphi_V \left(\vec{p}_b - \frac{\vec{q}_b}{2} \right) \\ & \times \sum_{r_1, r_2, s_1, s_2} w_{m'_1 m_1}^{q_1}(\vec{x}_1, \vec{p}_1) w_{m'_2 m_2}^{\bar{q}_2}(\vec{x}_2, \vec{p}_2) \\ & \times \langle j_V m' | m'_1 m'_2 \rangle \langle m_1 m_2 | j_V m \rangle, \end{aligned} \quad (36)$$

where $\vec{x}_{1,2} \equiv \vec{x} \pm \vec{x}_b/2$ and $\vec{p}_{1,2} \equiv \vec{p}/2 \pm \vec{p}_b$ are positions and momenta for the quark q_1 and the antiquark \bar{q}_2 respectively, and $N(\vec{x}, \vec{p})$ is the normalization factor that ensures $\sum_{m=0,\pm 1} \rho_{mm}^V(\vec{x}, \vec{p}) = 1$. Since we work in the non-relativistic limit, the spin and momentum can be decoupled. Therefore Clebsch-Gordan coefficients $\langle m_1 m_2 | j_V m \rangle$ and $\langle j_V m' | m'_1 m'_2 \rangle$ as well as the meson's wave function φ_V appear in Eq. (36). By further neglecting the phase-space dependence of unpolarized distribution functions and choosing φ_V as a Gaussian distribution with the width a_V in the momentum space, we derive the spin alignment and other parameters in the angular distribution (16),

$$\begin{aligned} \rho_{00}^V(\vec{x}, \vec{p}) &\approx \frac{1}{3} - \frac{2}{3} \langle P_{q_1}^z P_{\bar{q}_2}^z \rangle_V + \frac{2}{9} \langle \vec{P}_{q_1} \cdot \vec{P}_{\bar{q}_2} \rangle_V, \\ \text{Re} \rho_{1,-1}^V(\vec{x}, \vec{p}) &\approx \frac{1}{3} \langle P_{q_1}^x P_{\bar{q}_2}^x - P_{q_1}^y P_{\bar{q}_2}^y \rangle_V, \end{aligned}$$

$$- \text{Im} \rho_{1,-1}^V(\vec{x}, \vec{p}) \approx \frac{1}{3} \langle P_{q_1}^x P_{\bar{q}_2}^y + P_{q_1}^y P_{\bar{q}_2}^x \rangle_V,$$

$$\text{Re} [\rho_{1,0} - \rho_{-1,0}] (\vec{x}, \vec{p}) \approx \frac{\sqrt{2}}{3} \langle P_{q_1}^z P_{\bar{q}_2}^x + P_{q_1}^x P_{\bar{q}_2}^z \rangle_V,$$

$$- \text{Im} [\rho_{1,0} + \rho_{-1,0}] (\vec{x}, \vec{p}) \approx \frac{\sqrt{2}}{3} \langle P_{q_1}^y P_{\bar{q}_2}^z + P_{q_1}^z P_{\bar{q}_2}^y \rangle_V, \quad (37)$$

where the correlation between quark and antiquark's polarizations is defined as

$$\begin{aligned} \langle P_{q_1}^i P_{\bar{q}_2}^j \rangle_V &\equiv \frac{1}{\pi^3} \int d^3\vec{x}_b d^3\vec{p}_b \exp \left(-\frac{\vec{p}_b^2}{a_V^2} - a_V^2 \vec{x}_b^2 \right) \\ & \times P_{q_1}^i(\vec{x}_1, \vec{p}_1) P_{\bar{q}_2}^j(\vec{x}_2, \vec{p}_2). \end{aligned} \quad (38)$$

We note that in Eq. (37) the spin quantization direction is set to the z -direction.

2. Relativistic model in quantum kinetic approach

For a relativistic quark or antiquark, its polarization four-vector is always perpendicular to its four-momentum, implying that the spin with momentum cannot be decoupled as in the non-relativistic case. Consequently, the vector meson's spin cannot be obtained by the constituent quark's and anti-quark's spins through the angular momentum coupling in non-relativistic quantum mechanics. Based on the Kadanoff-Baym equation in the closed-time-path formalism, a relativistic spin kinetic theory for vector mesons has been constructed [38] to explain experimental data on the spin alignment [26].

In order to describe spin transport phenomena, we use the matrix-valued spin-dependent distribution (MVSD) $f_{m_1 m_2}^V(x, \vec{p})$ for the vector meson. The spin Boltzmann equation with coalescence and dissociation collision terms reads,

$$\begin{aligned} & p \cdot \partial_x f_{m_1 m_2}^V(x, \vec{p}) \\ &= \frac{1}{16} \sum_{m'_1, m'_2} [\epsilon_\mu^*(m_1, \vec{p}) \epsilon_\nu(m'_1, \vec{p}) \delta_{m_2 m'_2} \\ & + \delta_{m_1 m'_1} \epsilon_\mu^*(m'_2, \vec{p}) \epsilon_\nu(m_2, \vec{p})] \\ & \times \mathcal{C}_{m'_1 m'_2}^{\mu\nu}(x, \vec{p}), \end{aligned} \quad (39)$$

where $\epsilon^\mu(m, \vec{p})$ denotes the meson's normalized polarization vector perpendicular to p^μ , and m_1, m_2, m'_1 , and m'_2 label the vector meson's spin states along the spin quantization direction with three values 0 and ± 1 . Here we have assumed that the vector meson is on its mass-shell $p^0 = \sqrt{m_V^2 + \vec{p}^2}$. The gain and loss terms in $\mathcal{C}_{m'_1 m'_2}^{\mu\nu}$ correspond to the coalescence and dissociation processes for the quark and antiquark, respectively. In the dilute limit when distribution functions of the meson, the constituent quark and antiquark are much less than unity, Eq. (39) is simplified as

$$p \cdot \partial_x f_{m_1 m_2}^V(x, \vec{p}) = \frac{1}{8} [\epsilon_\mu^*(m_1, \vec{p}) \epsilon_\nu(m_2, \vec{p}) \mathcal{C}_{\text{coal}}^{\mu\nu}(x, \vec{p})$$

$$-\mathcal{C}_{\text{diss}}(\vec{p})f_{m_1 m_2}^V(x, \vec{p})], \quad (40)$$

where the contribution from the dissociation is proportional to the MVSD with the coefficient $\mathcal{C}_{\text{diss}}$ being independent of the MVSD. The coalescence kernel $\mathcal{C}_{\text{coal}}^{\mu\nu}$ can be obtained from the Kadanoff-Baym equation,

$$\begin{aligned} \mathcal{C}_{\text{coal}}^{\mu\nu}(x, \vec{p}) = & \int \frac{d^3\vec{p}'}{(2\pi)^2} \frac{\delta(E_{\vec{p}}^V - E_{\vec{p}'}^q - E_{\vec{p}-\vec{p}'}^q)}{E_{\vec{p}'}^q E_{\vec{p}-\vec{p}'}^q} \\ & \times \text{Tr} \{ \Gamma^\nu(p' \cdot \gamma - M_{\bar{q}}) \\ & \times [1 + \gamma_5 \gamma \cdot P_{\bar{q}}(x, \vec{p}')] \\ & \times \Gamma^\mu[(p - p') \cdot \gamma + M_q] \\ & \times [1 + \gamma_5 \gamma \cdot P_q(x, \vec{p} - \vec{p}')] \} \\ & \times f_{\bar{q}}(x, \vec{p}') f_q(x, \vec{p} - \vec{p}'), \end{aligned} \quad (41)$$

where M_q and $M_{\bar{q}}$ are quark and antiquark masses respectively, $E_{\vec{p}}^V$, $E_{\vec{p}-\vec{p}'}^q$, and $E_{\vec{p}'}^q$ are energies for the vector meson, the constituent quark and antiquark respectively, and Γ^μ is the effective vertex of quark-antiquark-meson. Here $f_{q/\bar{q}}$ and $P_{q/\bar{q}}^\mu$ are the unpolarized and spin polarization distributions for the quark/antiquark respectively. By neglecting the space dependence (the distributions are homogeneous in space) and setting $f_{m_1 m_2}^V = 0$ before the hadronization stage in heavy-ion collisions, one can obtain a formal solution to Eq. (40). Spin density matrix elements can be derived as [39],

$$\rho_{m_1 m_2}^V(x, \vec{p}) = \frac{\epsilon_\mu^*(m_1, \vec{p}) \epsilon_\nu(m_2, \vec{p}) \mathcal{C}_{\text{coal}}^{\mu\nu}(x, \vec{p})}{\sum_{m=0, \pm 1} \epsilon_\alpha^*(m, \vec{p}) \epsilon_\beta(m, \vec{p}) \mathcal{C}_{\text{coal}}^{\alpha\beta}(x, \vec{p})}. \quad (42)$$

This is a relativistic formula for the vector meson's spin density matrix built from the coalescence kernel (41) encoding the polarization distributions of the constituent quark and antiquark. Clearly the vector meson's spin density matrix has non-trivial dependence on the spin polarization and momenta of the quark and antiquark.

We consider that s and \bar{s} are polarized in a thermal medium by an effective vector field called the ϕ field [37–39] induced by currents of pseudo-Goldstone bosons [78]. The spin polarization of s and \bar{s} is then given by

$$P_{q/\bar{q}}^\mu(x, \vec{p}) \approx \pm \frac{g_\phi}{4M_s(u \cdot p)T_h} \epsilon^{\mu\nu\alpha\beta} p_\nu F_{\alpha\beta}^\phi(x), \quad (43)$$

where u^μ denotes the velocity of the thermal background at the effective hadronization temperature T_h , g_ϕ is the effective coupling constant of the $s\bar{s}\phi$ vertex, and $F_{\alpha\beta}^\phi(x)$ is the ϕ field's strength tensor. Substituting (43) into Eq. (41) and assuming $u^\mu = (1, 0, 0, 0)$ in the meson's rest frame, we obtain the spin alignment of the ϕ meson

$$\begin{aligned} \rho_{00}^\phi(x, \vec{p}) & \approx \frac{1}{3} - \frac{4g_\phi^2}{M_\phi^2 T_h} C_1 \left[\frac{1}{3} \vec{B}'_\phi \cdot \vec{B}'_\phi - (\vec{\epsilon}_0 \cdot \vec{B}'_\phi)^2 \right] \\ & - \frac{4g_\phi^2}{M_\phi^2 T_h} C_2 \left[\frac{1}{3} \vec{E}'_\phi \cdot \vec{E}'_\phi - (\vec{\epsilon}_0 \cdot \vec{E}'_\phi)^2 \right], \end{aligned} \quad (44)$$

where M_ϕ is the mass of the ϕ meson, and \vec{B}'_ϕ and \vec{E}'_ϕ are electric and magnetic components of the ϕ field in the meson's rest frame respectively. Here $\vec{\epsilon}_0$ denotes the spin quantization direction. The coefficients C_1 and C_2 depend only on quark's and meson's masses,

$$\begin{aligned} C_1 &= \frac{8M_s^4 + 16M_s^2 M_\phi^2 + 3M_\phi^4}{120M_s^2(M_\phi^2 + 2M_s^2)}, \\ C_2 &= \frac{8M_s^4 - 14M_s^2 M_\phi^2 + 3M_\phi^4}{120M_s^2(M_\phi^2 + 2M_s^2)}. \end{aligned} \quad (45)$$

We note that the momentum dependence can be obtained by expressing \vec{B}'_ϕ and \vec{E}'_ϕ in Eq. (44) in terms of laboratory frame fields through Lorentz transformation.

$$\begin{aligned} \vec{B}'_\phi &= \gamma \vec{B}_\phi - \gamma \vec{v} \times \vec{E}_\phi + (1 - \gamma) \frac{\vec{v} \cdot \vec{B}_\phi}{v^2} \vec{v}, \\ \vec{E}'_\phi &= \gamma \vec{E}_\phi + \gamma \vec{v} \times \vec{B}_\phi + (1 - \gamma) \frac{\vec{v} \cdot \vec{E}_\phi}{v^2} \vec{v}, \end{aligned} \quad (46)$$

where $\gamma = E_{\vec{p}}^\phi/M_\phi$ is the Lorentz factor and $\vec{v} = \vec{p}/E_{\vec{p}}^\phi$ is the velocity of the ϕ meson. Then ρ_{00}^ϕ can be rewritten as

$$\begin{aligned} \rho_{00}^\phi(x, \vec{p}) &\approx \frac{1}{3} - \frac{4g_\phi^2}{3M_\phi^4 T_h^2} \sum_{i=1,2,3} I_{B,i}(\vec{p}) (\vec{B}_i^\phi)^2 \\ &- \frac{4g_\phi^2}{3M_\phi^4 T_h^2} \sum_{i=1,2,3} I_{E,i}(\vec{p}) (\vec{E}_i^\phi)^2, \end{aligned} \quad (47)$$

where $I_{B,i}(\vec{p})$ and $I_{E,i}(\vec{p})$ are momentum functions. One can further take the space and momentum average of $\rho_{00}^\phi(x, \vec{p})$

$$\begin{aligned} \langle \rho_{00}^\phi(x, \vec{p}) \rangle_{x, \vec{p}} &\approx \frac{1}{3} - \frac{4g_\phi^2}{3M_\phi^4 T_h^2} \sum_{i=1,2,3} \langle I_{B,i}(\vec{p}) \rangle_{\vec{p}} \langle (\vec{B}_i^\phi)^2 \rangle_x \\ &- \frac{4g_\phi^2}{3M_\phi^4 T_h^2} \sum_{i=1,2,3} \langle I_{E,i}(\vec{p}) \rangle_{\vec{p}} \langle (\vec{E}_i^\phi)^2 \rangle_x, \end{aligned} \quad (48)$$

where the momentum average is defined as

$$\langle O(\vec{p}) \rangle_{\vec{p}} = \frac{\int d^3\vec{p}' (E_{\vec{p}'}^\phi)^{-1} O(\vec{p}') f_\phi(\vec{p}')}{\int d^3\vec{p}' (E_{\vec{p}'}^\phi)^{-1} f_\phi(\vec{p}')}, \quad (49)$$

if we want to obtain momentum-integrated data for ρ_{00}^ϕ . Here $f_\phi(\vec{p})$ is its momentum distribution which may contain information about collective flows such as v_1 and v_2 . If we want to obtain the transverse momentum spectra of ρ_{00}^ϕ , we have to integrate over the azimuthal angle and rapidity and keep p_T , i.e. to replace $d^3\vec{p}/E_p^\phi$ in (49) by $dy d\varphi$. We see in Eq. (49) that the average ρ_{00}^ϕ depends on the space average field squared which quantifies the field fluctuation. The theoretical results for $\langle \rho_{00}^\phi \rangle$ as functions of transverse momenta, collision energies and centralities are presented in Ref. [39], which are in a good agreement with recent STAR data [35].

V. LINEAR RESPONSE THEORY FOR SPIN ALIGNMENT OF VECTOR MESONS IN THERMAL MEDIA

In this section, we will show how to calculate the spin alignment of the vector meson from the Kubo formula in linear response theory [83–86] in thermalized QGP. The detailed discussion of this topic is in Ref. [75].

The Closed-Time-Path (CTP) formalism is a field-theory based method for many-particle systems in off-equilibrium as well in equilibrium [87–92]. When it is used for systems in equilibrium, it is actually the real time formalism of the thermal field theory [86, 93]. Wigner functions can be obtained from two-point Green's functions on the CTP [34, 38, 75, 94, 95]. The on-shell Wigner function for the vector meson is related to its MVSD (proportional to the spin density matrix) and defined as

$$\begin{aligned} W^{\mu\nu}(x, p_{\text{on}}) &= \frac{E_p}{\pi} \int_0^\infty dp_0 G_{<}^{\mu\nu}(x, p) \\ &= \sum_{m_1, m_2} \epsilon^\mu(m_1, \vec{p}) \epsilon^{\nu*}(m_2, \vec{p}) f_{m_1 m_2}^V(x, \vec{p}), \end{aligned} \quad (50)$$

where $G_{<}^{\mu\nu}(x, p)$ is the “+−” component of two-point Green's functions on the CTP, and $f_V = \text{Tr}(f_V) \hat{\rho}^V$ with $f_V \equiv f_{m_1 m_2}^V$ being the short-hand notation for the MVSD, $\text{Tr}(f_V) = \sum_m f_{mm}^V$ being the trace of the MVSD, and $\hat{\rho}_V$ being the spin density matrix in Eq. (2). One can check that $W^{\mu\nu}(x, p_{\text{on}})$ is always transverse to the on-shell momentum, $p_\mu^{\text{on}} W^{\mu\nu}(x, p_{\text{on}}) = 0$. The on-shell Wigner function can be decomposed into the scalar (\mathcal{S}), polarization ($W^{[\mu\nu]}$) and tensor polarization ($\mathcal{T}^{\mu\nu}$) parts as [34, 96]

$$\begin{aligned} W^{\mu\nu}(x, p_{\text{on}}) &= W^{[\mu\nu]} + W^{(\mu\nu)} \\ &= -\frac{1}{3} \Delta^{\mu\nu}(p_{\text{on}}) \mathcal{S} + W^{[\mu\nu]} + \mathcal{T}^{\mu\nu}, \end{aligned} \quad (51)$$

where each part is defined as

$$\begin{aligned} W^{[\mu\nu]} &\equiv \frac{1}{2} (W^{\mu\nu} - W^{\nu\mu}), \\ W^{(\mu\nu)} &\equiv \frac{1}{2} (W^{\mu\nu} + W^{\nu\mu}), \\ \mathcal{T}^{\mu\nu} &\equiv W^{(\mu\nu)} + \frac{1}{3} \Delta^{\mu\nu}(p_{\text{on}}) \mathcal{S}. \end{aligned} \quad (52)$$

With Eq. (51) one can show that both $W^{[\mu\nu]}$ and $\mathcal{T}^{\mu\nu}$ are traceless, $g_{\mu\nu} W^{[\mu\nu]} = g_{\mu\nu} \mathcal{T}^{\mu\nu} = 0$. Using Eqs. (2) and (50), we obtain

$$\begin{aligned} \mathcal{S} &= \text{Tr}(f_V) = -\Delta^{\mu\nu}(p_{\text{on}}) W_{\mu\nu}, \\ W^{[\mu\nu]} &= \frac{1}{2} \text{Tr}(f_V) \sum_{\lambda_1, \lambda_2} \epsilon^\mu(\lambda_1, \vec{p}) \epsilon^{\nu*}(\lambda_2, \vec{p}) P_i \Sigma_{\lambda_1 \lambda_2}^i, \\ \mathcal{T}^{\mu\nu} &= \text{Tr}(f_V) \sum_{\lambda_1, \lambda_2} \epsilon^\mu(\lambda_1, \vec{p}) \epsilon^{\nu*}(\lambda_2, \vec{p}) T_{ij} \Sigma_{\lambda_1 \lambda_2}^{ij}. \end{aligned} \quad (53)$$

We see that $W^{[\mu\nu]}$ is related to P_i while $\mathcal{T}^{\mu\nu}$ is related to T_{ij} .

We can extract $f_{00} \propto \rho_{00}$ by projecting

$$L^{\mu\nu}(p_{\text{on}}) = \epsilon^{\mu,*}(0, \vec{p}) \epsilon^\nu(0, \vec{p}) + \frac{1}{3} \Delta^{\mu\nu}(p_{\text{on}}), \quad (54)$$

onto $W^{\mu\nu}$ in Eq. (50) as

$$\begin{aligned} L_{\mu\nu}(p_{\text{on}}) W^{\mu\nu} &= \sum_{\lambda_1, \lambda_2} L_{\mu\nu}(p_{\text{on}}) \epsilon^\mu(\lambda_1, \vec{p}) \epsilon^{\nu*}(\lambda_2, \vec{p}) f_{\lambda_1 \lambda_2}^V(x, \vec{p}) \\ &= f_{00}^V(x, \vec{p}) + \frac{1}{3} \sum_{\lambda_1, \lambda_2} \epsilon^\mu(\lambda_1, \vec{p}) \epsilon_\mu^*(\lambda_2, \vec{p}) f_{\lambda_1 \lambda_2}^V(x, \vec{p}) \\ &= f_{00}^V(x, \vec{p}) - \frac{1}{3} \text{Tr}(f_V). \end{aligned} \quad (55)$$

In (54), $\epsilon^\mu(0, \vec{p})$ is the polarization vector along the spin quantization direction. With the first line of Eq. (53) and Eq. (55), we obtain

$$\frac{L_{\mu\nu}(p_{\text{on}}) W^{\mu\nu}}{-\Delta^{\mu\nu}(p_{\text{on}}) W_{\mu\nu}} = \frac{f_{00}^V(x, \vec{p})}{\text{Tr}[f_V(x, \vec{p})]} - \frac{1}{3} = \rho_{00} - \frac{1}{3}. \quad (56)$$

The above formula relates the Wigner function to ρ_{00} .

The medium effects can be described by retarded and advanced two-point Green's functions through spectral functions. For vector mesons interacting with thermal quarks, the spectral function can be defined through the imaginary part of the retarded two-point Green's function (propagator in momentum space) as

$$\text{Im} \tilde{G}_R^{\mu\nu}(p) = \Delta_T^{\mu\nu} \rho_T(p) + \Delta_L^{\mu\nu} \rho_L(p). \quad (57)$$

The definition of two-point Green's functions G and Σ differs by a factor $i = \sqrt{-1}$ from the usual one in quantum field theory, which are related by $G = i \tilde{G}$ and $\Sigma = i \tilde{\Sigma}$. In Eq. (57), we defined

$$\begin{aligned} \Delta_T^{\mu\nu} &= -g^{\mu 0} g^{\nu 0} + g^{\mu\nu} + \frac{\mathbf{p}^\mu \mathbf{p}^\nu}{|\vec{p}|^2}, \\ \Delta_L^{\mu\nu} &= \Delta^{\mu\nu} - \Delta_T^{\mu\nu} \equiv g^{\mu\nu} - \frac{p^\mu p^\nu}{p^2} - \Delta_T^{\mu\nu}, \end{aligned} \quad (58)$$

as the transverse and longitudinal projector respectively with $\mathbf{p}^\mu = (0, \vec{p})$, and $\rho_{T,L}$ are spectral functions in the transverse and longitudinal directions given by [75]

$$\begin{aligned} \rho_T(p) &= -\text{Im} \frac{1}{p^2 - m^2 + \tilde{\Sigma}_\perp(p) + i \text{sgn}(p_0) \varepsilon}, \\ \rho_L(p) &= -\text{Im} \frac{1}{p^2 - m^2 + \frac{p^2}{|\vec{p}|^2} \tilde{\Sigma}_{00}(p) + i \text{sgn}(p_0) \varepsilon}, \end{aligned} \quad (59)$$

where $\tilde{\Sigma}_\perp$ and $\tilde{\Sigma}_{00}$ are from $\tilde{\Sigma}_R^{\mu\nu}$: $\tilde{\Sigma}_\perp \equiv -(1/2) \Delta_{\mu\nu}^T \tilde{\Sigma}_R^{\mu\nu}$ and $\tilde{\Sigma}_{00} = \tilde{\Sigma}_R^{00}$, $\text{sgn}(p_0)$ is the sign of p_0 , and ε is an infinitesimal positive number. One can check in Eq. (58) that $p_\mu \Delta_T^{\mu\nu} = p_\mu \Delta_L^{\mu\nu} = 0$. In Eq. (59), one can verify

that the real parts of $\tilde{\Sigma}_\perp$ and $\tilde{\Sigma}_{00}$ contribute to the mass correction while the imaginary parts of $\tilde{\Sigma}_\perp$ and $\tilde{\Sigma}_{00}$ determine the width or life-time of the quasi-particle mode.

The two-point function $G_{<}^{\mu\nu}$ is related to $G_A^{\mu\nu}$ and $G_R^{\mu\nu}$ through [84, 97]

$$\begin{aligned} G_{<}^{\mu\nu}(p) &= in_B(p_0) \left[\tilde{G}_R^{\mu\nu}(p) - \tilde{G}_A^{\mu\nu}(p) \right] \\ &= -2n_B(p_0) \text{Im} \tilde{G}_R^{\mu\nu}(p), \end{aligned} \quad (60)$$

where $n_B(p_0) = 1/(e^{\beta p_0 - \beta \mu_V} - 1)$ is the Bose-Einstein distribution with the inverse temperature $\beta \equiv 1/T$ and the vector meson's chemical potential μ_V . Inserting Eq. (60) into (50) we obtain the on-shell Wigner function $W^{\mu\nu}(p_{\text{on}})$ from which the spin alignment ρ_{00} can be extracted through Eq. (56).

For free vector mesons, the spectral functions are $\rho_T^{(0)} = \rho_L^{(0)} = \pi \text{sgn}(p_0) \delta(p^2 - m^2)$, which give $G_{<}^{\mu\nu}(p)$ and $\text{Im} \tilde{G}_R^{\mu\nu}(p)$ for the free vector meson following Eqs. (57) and (60).

The non-equilibrium correction to $G_{<}^{\mu\nu}(p)$ can be calculated through the Kubo formula in linear response theory. The Kubo formula has been derived in Zubarev's approach to non-equilibrium density operator [85, 98, 99]. Detailed derivation is given in Ref. [99]. Considering the thermal shear tensor $\xi_{\mu\nu} = 1/2(\partial_\mu \beta_\nu + \partial_\nu \beta_\mu)$ as a perturbation from local equilibrium, the next-to-leading order correction of $G_{<}^{\mu\nu}$ can be written as [75]

$$\begin{aligned} \delta G_{<}^{\mu\nu}(x, p) &= 4T \lim_{K^\mu \rightarrow 0} \frac{\partial}{\partial K_0} \text{Im} \int \frac{dp_1^0 dp_2^0}{2\pi} \\ &\times \frac{n_B(p_1^0) - n_B(p_2^0)}{p_1^0 - p_2^0 + K^0 + i\epsilon} \delta \left(p^0 - \frac{p_1^0 + p_2^0}{2} \right) \xi_{\gamma\lambda} \\ &\times \sum_{a,b=L,T} \rho_a(p_1) \rho_b(p_2) I_{ab}^{\mu\nu\gamma\lambda}(p_1, p_2), \end{aligned} \quad (61)$$

where $p_1 = (p_1^0, \vec{p} - \vec{K}/2)$, $p_2 = (p_2^0, \vec{p} + \vec{K}/2)$. The tensor $I_{ab}^{\mu\nu\gamma\lambda}(p_1, p_2)$ is expressed as [75]

$$\begin{aligned} I_{ab}^{\mu\nu\gamma\lambda}(p_1, p_2) &= (p_1^\lambda p_2^\gamma + p_1^\gamma p_2^\lambda) \Delta_{a,\alpha}^\nu(p_1) \Delta_b^{\mu\alpha}(p_2) \\ &+ (p_{1,\alpha} p_2^\alpha - m_V^2) \\ &\times \left[\Delta_a^{\gamma\nu}(p_1) \Delta_b^{\mu\lambda}(p_2) + \Delta_a^{\lambda\nu}(p_1) \Delta_b^{\mu\gamma}(p_2) \right] \\ &- \left[p_1^\gamma p_2^\alpha \Delta_{a,\alpha}^\nu(p_1) \Delta_b^{\mu\lambda}(p_2) \right. \\ &+ p_2^\gamma p_1^\alpha \Delta_a^{\lambda\nu}(p_1) \Delta_{b,\alpha}^\mu(p_2) \\ &- \left[p_{1,\alpha} p_2^\lambda \Delta_a^{\gamma\nu}(p_1) \Delta_b^{\mu\alpha}(p_2) \right. \\ &+ p_1^\lambda p_{2,\alpha} \Delta_a^{\alpha\nu}(p_1) \Delta_b^{\mu\gamma}(p_2) \\ &- g^{\gamma\lambda} [g_{\beta\alpha} (p_{2,\rho} p_1^\rho - m_V^2) - p_{1,\beta} p_{2,\alpha}] \\ &\times \Delta_a^{\alpha\nu}(p_1) \Delta_b^{\mu\beta}(p_2), \end{aligned} \quad (62)$$

where $\Delta_T^{\mu\nu}(p)$ and $\Delta_L^{\mu\nu}(p)$ are given by Eq. (58). Then the spin alignment of vector mesons can be obtained from Eq. (56) through Eqs. (50) and (61).

Under the quasi-particle approximation (QPA), the self-energies and spectral functions can be calculated analytically by expanding p_0 in powers of $\delta p_0 = p_0 - E_p^V$. This expansion requires $\Delta E/E_p^V \sim \Gamma/E_p^V \sim \epsilon \ll 1$, where ΔE and Γ are the mass shift and width of the vector meson respectively. Then the spin alignment can be expressed as

$$\delta \rho_{00}(\vec{p}) = \delta \rho_{00}^{(\xi=0)}(\vec{p}) + \xi_{\mu\nu} C^{\mu\nu}(\vec{p}), \quad (63)$$

where $\delta \rho_{00}^{(\xi=0)}$ is the spin alignment independent of the shear stress tensor and $C^{\mu\nu}$ is the dimensionless tensor coefficient in the shear stress term. The results under the QPA are compared with full numerical results are shown in Fig. (4). For the values of parameters we choose, the magnitudes of $\delta \rho_{00}^{(\xi=0)}$ and $C^{\mu\nu}(\vec{p})$ are $\mathcal{O}(10^{-3})$ and $\mathcal{O}(10^{-2} \sim 10^{-3})$, respectively. As a consequence, if the thermal shear tensor is $\mathcal{O}(10^{-2})$, the contribution from the thermal shear tensor to the ϕ meson's spin alignment is $\mathcal{O}(10^{-4} \sim 10^{-5})$, which is much smaller than the contribution from the strong force fields [39].

VI. VECTOR MESON'S SPIN ALIGNMENTS IN QUARK FRAGMENTATION

In high energy reactions, hadron production is normally described by fragmentation functions (FFs). The hadron's Polarization can be realized in terms of polarized FFs [56–58]. These FFs are defined via quark-quark correlators. Among different high energy reactions, the clean and ideal place to study FFs is in high energy e^+e^- collisions. In Ref. [56], the complete decomposition of quark-quark correlators for spin-1 hadrons with systematic results for hadron polarization in terms of FFs up to twist-3 in $e^+e^- \rightarrow V\pi X$ have been presented. Experimental measurements have been carried out many years ago for the longitudinal polarization of Λ hyperons [67, 68] and for the spin alignments of vector mesons [46–49] in the inclusive production process $e^+e^- \rightarrow hX$ at LEP. Significant effects have been observed. These experimental data have attracted many phenomenological studies [51–58] and parameterization of corresponding FFs has been obtained [56–58]. In this section we will summarize these results.

A. FFs from quark-quark correlator

For the fragmentation of the quark (or anti-quark), the quark-quark correlator as a 4×4 matrix in Dirac indices is defined by

$$\hat{\Xi}(k; p, S) = \sum_X \int \frac{d^4\xi}{2\pi} e^{-ik\xi} \langle hX | \bar{\psi}(\xi) \mathcal{L}(\xi; \infty) | 0 \rangle$$

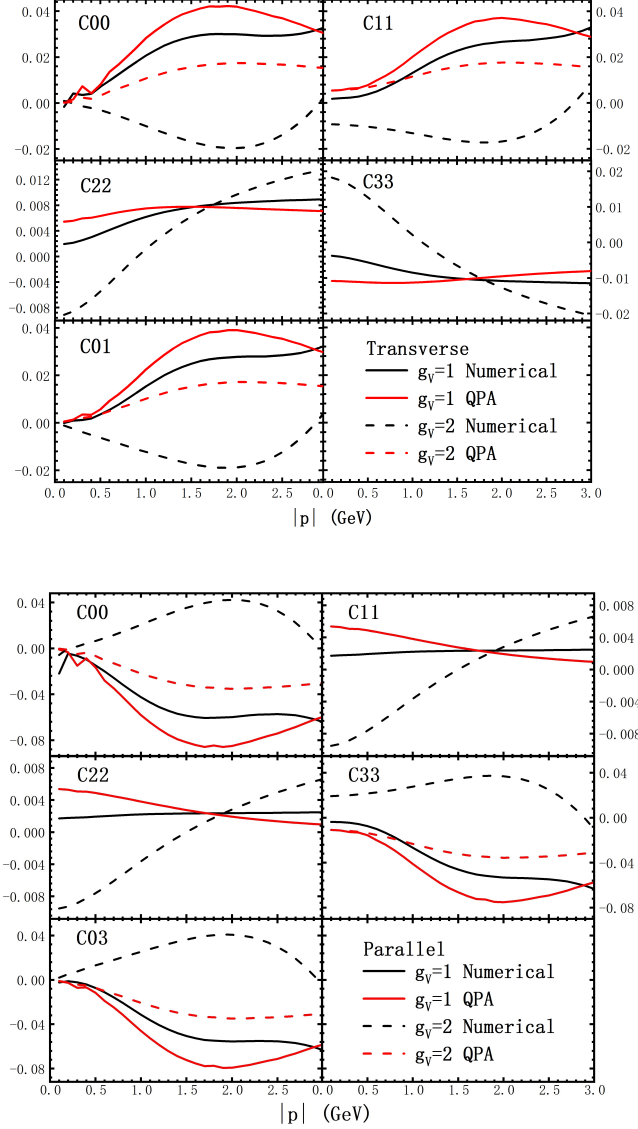


FIG. 4. The full numerical and QPA results for $C^{\mu\nu}$ as functions of vector mesons' momenta. In the upper panel the momentum is perpendicular to the spin quantization direction z , while in the lower panel the momentum is parallel to the spin quantization direction.

$$\times \langle 0 | \mathcal{L}^\dagger(0; \infty) \psi(0) | hX \rangle, \quad (64)$$

where k and p are four-momenta of the quark and hadron respectively, S denotes the hadron's spin, and $\mathcal{L}(\xi; \infty)$ is the gauge link defined as

$$\mathcal{L}(\xi; \infty) = P \exp \left[ig \int_{\xi^-}^{\infty} d\eta^- A^+(\eta^-; \xi^+, \vec{\xi}_\perp) \right], \quad (65)$$

which guarantees the gauge invariance of FFs. In the rest part of the paper, for notational simplicity, we suppress the gauge link in forthcoming equations. In this case, the field operator $\psi(\xi)$ just stands for $\mathcal{L}^\dagger(\xi; \infty) \psi(\xi)$.

The FFs are obtained from $\hat{\Xi}(k; p, S)$ in the following way. First, we expand $\hat{\Xi}(k; p, S)$ in terms of Γ matrices as

$$\begin{aligned} \hat{\Xi}(k; p, S) = & \frac{1}{2} \left[\Xi(k; p, S) + i\gamma_5 \tilde{\Xi}(k; p, S) \right. \\ & + \gamma^\alpha \Xi_\alpha(k; p, S) + \gamma_5 \gamma^\alpha \tilde{\Xi}_\alpha(k; p, S) \\ & \left. + i\sigma^{\alpha\beta} \gamma_5 \Xi_{\alpha\beta}(k; p, S) \right], \end{aligned} \quad (66)$$

where coefficients are all real functions and are Lorentz scalar, pseudo-scalar, vector, axial-vector and tensor respectively. Then we expand these coefficient functions according to their respective Lorentz transformation properties in terms of basic Lorentz covariants multiplied by scalar functions which are constructed from available variables. These scalar functions are the FFs.

Clearly, basic Lorentz covariants to be constructed depend strongly on what variables that we have at hand. Besides p and k , we have variables for spin states which are different for spin-0, 1/2 or 1 hadrons. For this purpose, we need to decompose the spin density matrix in terms of known operators multiplied by Lorentz covariants. For spin-1/2 hadrons, the spin density matrix ρ is decomposed as in Eq. (1), but \vec{S} in the rest frame of the hadron should be generalized to a covariant form $S = (0, \vec{S})$. For spin-1 hadrons, the 3×3 density matrix $\hat{\rho}$ is usually decomposed as in Eq. (2). The tensor polarization $T^{ij} = \text{Tr}(\rho \Sigma^{ij})$ can be parameterized as

$$[T] = \frac{1}{2} \begin{pmatrix} -\frac{2}{3} S_{LL} + S_{TT}^{xx} & S_{TT}^{xy} & S_{LT}^x \\ S_{TT}^{xy} & -\frac{2}{3} S_{LL} - S_{TT}^{xx} & S_{LT}^y \\ S_{LT}^x & S_{LT}^y & \frac{4}{3} S_{LL} \end{pmatrix}. \quad (67)$$

We see that, for spin-1 hadrons, besides the polarization vector S , there is also a tensor polarization part. The polarization vector is similar to that for spin-1/2 hadrons. The tensor polarization part has five components, namely a Lorentz scalar S_{LL} , a Lorentz vector $S_{LT}^\mu = (0, S_{LT}^x, S_{LT}^y, 0)$ and a Lorentz tensor $S_{TT}^{\mu\nu}$ that has two components $S_{TT}^{xx} = -S_{TT}^{yy}$ and $S_{TT}^{xx} = S_{TT}^{yy}$. The vector meson's spin alignment ρ_{00} is only related to S_{LL} through $\rho_{00} = (1 - 2S_{LL})/3$.

The quark-quark correlator given by Eq. (64) is un-integrated, i.e. it depends on the four-momentum k . If we consider three- or one-dimensional FFs, we need to integrate it over k^- and \vec{k}_\perp . We take one-dimensional FFs as an example. In this case, after integrating over k^- and \vec{k}_\perp , we obtain,

$$\begin{aligned} \hat{\Xi}(z; p, S) = & \sum_X \int \frac{d\xi^-}{2\pi} e^{-ik^+ \xi^-} \\ & \times \langle hX | \bar{\psi}(\xi^-) | 0 \rangle \langle 0 | \psi(0) | hX \rangle, \end{aligned} \quad (68)$$

where $z \equiv p^+/k^+$. After Lorentz decomposition, we obtain terms related to S_{LL} as,

$$z \Xi_\alpha(z; p, S) = p^+ \bar{n}_\alpha [D_1(z) + S_{LL} D_{1LL}(z)] +$$

+ power suppressed terms. (69)

We can obtain the expression for $D_1(z) + S_{LL}D_{1LL}(z)$ by reversely solving Eqs. (68) and (69),

$$D_1(z) + S_{LL}D_{1LL}(z) = \sum_X \int \frac{zd\xi^-}{2\pi p^+} e^{-ik^+\xi^-} \times \langle hX | \bar{\psi}(\xi^-) \gamma^+ | 0 \rangle \langle 0 | \psi(0) | hX \rangle, \quad (70)$$

For comparison, we present the corresponding equations for G_{1L} that describes the longitudinal spin transfer in the fragmentation process

$$z\tilde{\Xi}_\alpha(z; p, S) = \lambda p^+ \bar{n}_\alpha G_{1L}(z) + \text{power suppressed terms} \\ \lambda G_{1L}(z) = \sum_X \int \frac{zd\xi^-}{2\pi p^+} e^{-ik^+\xi^-} \times \langle hX | \bar{\psi}(\xi^-) \gamma^+ \gamma_5 | 0 \rangle \langle 0 | \psi(0) | hX \rangle. \quad (71)$$

The difference between $D_1(z) + S_{LL}D_{1LL}(z)$ in Eq. (70) and λG_{1L} in Eq. (71) is that γ^+ is involved in the former while $\gamma^+ \gamma_5$ is involved in the latter.

B. Vector meson's spin alignments from FFs

From Eqs. (70), we see clearly that, similar to the well-known unpolarized FF $D_1(z)$, D_{1LL} is independent of the quark's polarization because it is a sum over the quark's spin states

$$D_1(z) + S_{LL}D_{1LL}(z) = \sum_X \int \frac{zd\xi^-}{2\pi p^+} e^{-ik^+\xi^-} \times \sum_{\lambda_q=L,R} \langle hX | \bar{\psi}_{\lambda_q}(\xi^-) \gamma^+ | 0 \rangle \langle 0 | \psi_{\lambda_q}(0) | hX \rangle, \quad (72)$$

where $\lambda_q = L, R$ denotes the quark's helicity (or chirality), and $\psi_{L/R} = (1 \pm \gamma_5)\psi/2$. In contrast, the result for G_{1L} gives

$$\lambda G_{1L}(z) = \sum_X \int \frac{zd\xi^-}{2\pi p^+} e^{-ik^+\xi^-} \times [\langle hX | \bar{\psi}_L(\xi^-) \gamma^+ | 0 \rangle \langle 0 | \psi_L(0) | hX \rangle - \langle hX | \bar{\psi}_R(\xi^-) \gamma^+ | 0 \rangle \langle 0 | \psi_R(0) | hX \rangle], \quad (73)$$

which depends on the quark's spin explicitly.

We can draw an important conclusion from Eq. (72) for the spin alignment $\rho_{00} = (1 - 2S_{LL})/3$ for the vector meson produced in the fragmentation process $q \rightarrow VX$: it is determined by D_{1LL} and independent of the initial polarization of the quark. The conclusion is rather unexpected because the vector meson's spin alignment in high energy reactions was first observed in $e^+e^- \rightarrow VX$ at LEP [46–49] where initial quarks and anti-quarks are longitudinally polarized. However, this is consistent with space reflection in fragmentation processes where ρ_{00} is space reflection invariant while the helicity of the initial

quark changes the sign. This conclusion is rather solid since it follows from the general principle of QCD. It can also be tested easily in experiments. In the following we present numerical results for $e^+e^- \rightarrow VX$ and $pp \rightarrow VX$ as examples.

C. Vector meson's spin alignments in $e^+e^- \rightarrow VX$

Suppose that the quark fragmentation mechanism dominates hadron production in e^+e^- annihilation at high energies, we obtain the vector meson's alignment in $e^+e^- \rightarrow VX$ as

$$\langle S_{LL} \rangle(z, y) = \frac{\sum_q W_q(y) D_{1LL}(z)}{2 \sum_q W_q(y) D_1(z)}, \quad (74)$$

$$\langle \lambda \rangle(z, y) = \frac{\sum_q P_q(y) W_q(y) G_{1L}(z)}{\sum_q W_q(y) D_1(z)}, \quad (75)$$

where we also show the result of hyperon polarization for comparison. In Eqs. (74) and (75), $P_q(y)$ and $W_q(y)$ are the quark polarization and production weight at the vertex of e^+e^- annihilation respectively which are determined by the quark's electric charge, c_V^e and c_A^e in the weak interaction current, and so on (see e.g. [57] for the detailed expressions), $y = l_2 \cdot p_q / [(l_1 + l_2) \cdot p_q]$, where l_1 and l_2 are the four-momenta of the incident e^- and e^+ respectively, and p_q is the four-momentum of the produced quark.

The FFs are extracted from data available at a given scale and their scale dependence is determined by the QCD evolution equation, the DGLAP equation [100–107]. In Ref. [57, 58], such parameterizations of D_{1LL} for vector mesons have been obtained for the first time by fitting available data [46–48]. As comparison, parameterizations of G_{1L} for Λ are also given therein [57, 58] by fitting the LEP data [67, 68]. Here, we show the fitted results obtained there [57, 58] in Figs. 5 and 6.

From Figs. 5 and 6, we see a distinct feature that there is a strong energy dependence for $P_{L\Lambda}$, while the energy dependence for $\rho_{00}^{K^*}$ is weak. The former comes mainly from the energy dependence of P_q while the latter comes mainly from the QCD evolution of FFs. The relatively rapid change in the energy region around the mass of Z boson comes from the influence of W_q . This feature can be tested in future experiments.

D. Vector meson's spin alignments in $pp \rightarrow VX$

Assuming the universality of FFs, one can calculate vector meson's spin alignments in other high energy reactions where the fragmentation mechanism dominates. This applies to hadron production at high transverse momentum in pp collisions and deeply inelastic scatterings. In Ref. [58], such calculations have been carried out in pp collisions. As examples, we show in Fig. 7 the results

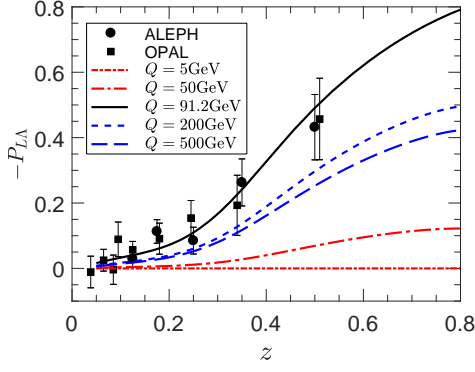


FIG. 5. Longitudinal polarization of Λ in $e^+e^- \rightarrow \Lambda X$ at high energies. The LEP data are taken from Refs. [67, 68]. The solid line is the fit obtained in Ref. [57] at the LEP energy while those at other energies are calculated results using the DGLAP equation for FFs and energy dependence of P_q . The figure is taken from Ref. [57].

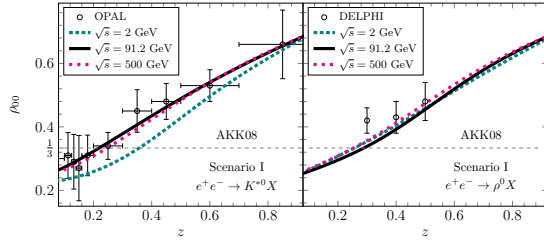


FIG. 6. The spin alignments of K^{*0} and ρ^0 in $e^+e^- \rightarrow VX$ at the Z-pole fitted in Ref. [58] compared with experimental data [46, 47]. The solid line is the fit in Ref. [58] at the LEP energy while those at other energies are the results using the DGLAP equation for FFs. The figure is taken from Ref. [57].

obtained there for K^{*0} and ρ^0 in two rapidity regions as functions of p_T .

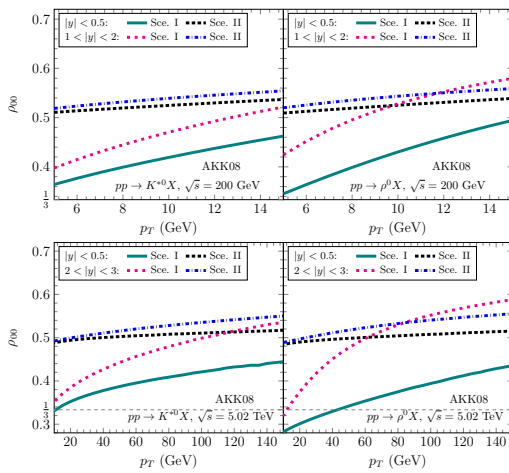


FIG. 7. Spin alignments of vector mesons in pp collisions at $\sqrt{s} = 200$ GeV and $\sqrt{s} = 5.02$ TeV for K^{*0} and ρ^0 in two rapidity regions as functions of p_T . This figure is taken from Ref. [58].

We see that ρ_{00}^V for vector mesons deviate from $1/3$ significantly showing large spin alignments. Such results can be tested in experiments at RHIC and LHC.

VII. SUMMARY AND OUTLOOK

Spin alignments for vector mesons have been observed in high energy reactions [35, 46–50]. There are two types of spin alignments: global spin alignments in heavy-ion collisions [35] and helicity-basis spin alignments in e^+e^- collisions [46–49]. These measurements show different features of spin alignments arising from different hadronization mechanisms in collisions of heavy-ion and e^+e^- .

In high energy heavy-ion collisions in the region of central rapidity and small transverse momentum, hadron production is mainly through quark combination or coalescence. The global spin alignment in this case not only depends on the polarization of quarks and anti-quarks but is also sensitive to the local correlation between the polarization of quarks and that of anti-quarks. Measurements of the global spin alignment in this case provide a good opportunity to study the polarization correlation in the sQGP produced in heavy-ion collisions. The STAR's measurements of ϕ meson's spin alignments [35] is consistent with the theoretical description based on ϕ vector fields that lead to a strong local correlation between P_s and $P_{\bar{s}}$ [36, 38, 39, 79]. The data were used to extract the strength of the local fluctuation in ϕ vector fields [38, 39].

In e^+e^- and pp collisions at high energies, hadron production is dominated by fragmentation with fragmentation functions. It has been shown that the spin alignment of vector mesons in the helicity basis is independent of the polarization of the initial quark in the quark fragmentation process. With the parameterization of corresponding fragmentation functions the prediction on spin alignments of vector mesons in high energy e^+e^- and pp collisions has been made [56–58].

It is impressive and interesting to see the distinction between the global spin alignments in high energy heavy-ion collisions and in e^+e^- or pp collisions which are dominated by different hadronization mechanisms. It is important to extend the measurements to different high energy reactions at different energies to test the universality of these properties. Obviously such studies provide new insights into properties of sQGP and hadronization mechanisms.

ACKNOWLEDGEMENTS

This work was supported in part by the National Key Research and Development Program of China under Contract No. 2022YFA1604900, by the National Natural Science Foundation of China (NSFC) under Contract Nos. 12025501, 11890710, 11890713, 11890714, 12147101 and

12135011, and by the Strategic Priority Research Pro-

gram of the Chinese Academy of Sciences (CAS) under Grant No. XDB34030102.

-
- [1] P. Braun-Munzinger, V. Koch, T. Schäfer, and J. Stachel, Phys. Rept. **621**, 76 (2016), 1510.00442.
 - [2] W. Florkowski, A. Kumar, and R. Ryblewski, Prog. Part. Nucl. Phys. **108**, 103709 (2019), 1811.04409.
 - [3] C. M. Ko, Nucl. Sci. Tech. **34**, 80 (2023).
 - [4] R. Rapp, Nucl. Sci. Tech. **34**, 63 (2023).
 - [5] Y. Zhang, D. W. Zhang, and X. F. Luo, Nucl. Tech. **46**, 040001 (2023).
 - [6] J. Zhao, J.-H. Chen, X.-G. Huang, and Y.-G. Ma, Nucl. Sci. Tech. **35**, 20 (2024).
 - [7] A. Pandav, D. Mallick, and B. Mohanty, Prog. Part. Nucl. Phys. **125**, 103960 (2022), 2203.07817.
 - [8] W.-B. He, Y.-G. Ma, L.-G. Pang, H.-C. Song, and K. Zhou, Nucl. Sci. Tech. **34**, 88 (2023).
 - [9] J. Chen, X. Dong, Y.-G. Ma, and Z. Xu, Sci. Bull. **68**, 3252 (2023), 2311.09877.
 - [10] Y. G. Ma, Nucl. Sci. Tech. **34**, 97 (2023).
 - [11] L. G. Pang and X. N. Wang, Nucl. Sci. Tech. **34**, 194 (2023).
 - [12] K. J. Sun *et al.*, Nucl. Tech. **46**, 040012 (2023).
 - [13] Q. Chen, G. L. Ma, and J. H. Chen, Nucl. Tech. **46**, 040013 (2023).
 - [14] Z.-T. Liang and X.-N. Wang, Phys. Rev. Lett. **94**, 102301 (2005), nucl-th/0410079, [Erratum: Phys.Rev.Lett. 96, 039901 (2006)].
 - [15] Z.-T. Liang and X.-N. Wang, Phys. Lett. B **629**, 20 (2005), nucl-th/0411101.
 - [16] S. A. Voloshin, (2004), nucl-th/0410089.
 - [17] B. Betz, M. Gyulassy, and G. Torrieri, Phys. Rev. C **76**, 044901 (2007), 0708.0035.
 - [18] A. Ipp, A. Di Piazza, J. Evers, and C. H. Keitel, Phys. Lett. B **666**, 315 (2008), 0710.5700.
 - [19] F. Becattini, F. Piccinini, and J. Rizzo, Phys. Rev. C **77**, 024906 (2008), 0711.1253.
 - [20] Z.-t. Liang, J. Phys. G **34**, S323 (2007), 0705.2852.
 - [21] STAR, J. H. Chen, J. Phys. G **34**, S331 (2007).
 - [22] J.-H. Gao *et al.*, Phys. Rev. C **77**, 044902 (2008), 0710.2943.
 - [23] STAR, I. Selyuzhenkov, J. Phys. G **34**, S1099 (2007), nucl-ex/0701034.
 - [24] STAR, B. I. Abelev *et al.*, Phys. Rev. C **77**, 061902 (2008), 0801.1729.
 - [25] STAR, B. I. Abelev *et al.*, Phys. Rev. C **76**, 024915 (2007), 0705.1691, [Erratum: Phys.Rev.C 95, 039906 (2017)].
 - [26] STAR, L. Adamczyk *et al.*, Nature **548**, 62 (2017), 1701.06657.
 - [27] Q. Wang, Nucl. Phys. A **967**, 225 (2017), 1704.04022.
 - [28] Z.-T. Liang, M. A. Lisa, and X.-N. Wang, Nucl. Phys. News **30**, 10 (2020), 1912.07822.
 - [29] J.-H. Gao, Z.-T. Liang, Q. Wang, and X.-N. Wang, Lect. Notes Phys. **987**, 195 (2021), 2009.04803.
 - [30] X.-G. Huang, J. Liao, Q. Wang, and X.-L. Xia, Lect. Notes Phys. **987**, 281 (2021), 2010.08937.
 - [31] J.-H. Gao, G.-L. Ma, S. Pu, and Q. Wang, Nucl. Sci. Tech. **31**, 90 (2020), 2005.10432.
 - [32] F. Becattini and M. A. Lisa, Ann. Rev. Nucl. Part. Sci. **70**, 395 (2020), 2003.03640.
 - [33] F. Becattini, Rept. Prog. Phys. **85**, 122301 (2022), 2204.01144.
 - [34] F. Becattini *et al.*, (2024), 2402.04540.
 - [35] STAR, M. S. Abdallah *et al.*, Nature **614**, 244 (2023), 2204.02302.
 - [36] Y.-G. Yang, R.-H. Fang, Q. Wang, and X.-N. Wang, Phys. Rev. C **97**, 034917 (2018), 1711.06008.
 - [37] X.-L. Sheng, L. Oliva, and Q. Wang, Phys. Rev. D **101**, 096005 (2020), 1910.13684, [Erratum: Phys.Rev.D 105, 099903 (2022)].
 - [38] X.-L. Sheng, L. Oliva, Z.-T. Liang, Q. Wang, and X.-N. Wang, Phys. Rev. D **109**, 036004 (2024), 2206.05868.
 - [39] X.-L. Sheng, L. Oliva, Z.-T. Liang, Q. Wang, and X.-N. Wang, Phys. Rev. Lett. **131**, 042304 (2023), 2205.15689.
 - [40] X.-N. Wang, Nucl. Sci. Tech. **34**, 15 (2023), 2302.00701.
 - [41] J. Chen, Z.-T. Liang, Y.-G. Ma, and Q. Wang, Sci. Bull. **68**, 874 (2023), 2305.09114.
 - [42] X.-L. Sheng, Z.-T. Liang, and Q. Wang, Acta Phys. Sin. **72**, 072502 (2023).
 - [43] J.-H. Gao, X.-G. Huang, Z.-T. Liang, Q. Wang, and X.-N. Wang, Acta Phys. Sin. **72**, 072501 (2023).
 - [44] L.-J. Ruan, Z.-B. Xu, and C. Yang, Acta Phys. Sin. **72**, 112401 (2023).
 - [45] J. Chen *et al.*, Nucl. Phys. News **34**, 17 (2024).
 - [46] DELPHI, P. Abreu *et al.*, Phys. Lett. B **406**, 271 (1997).
 - [47] OPAL, K. Ackerstaff *et al.*, Phys. Lett. B **412**, 210 (1997), hep-ex/9708022.
 - [48] OPAL, K. Ackerstaff *et al.*, Z. Phys. C **74**, 437 (1997).
 - [49] OPAL, G. Abbiendi *et al.*, Eur. Phys. J. C **16**, 61 (2000), hep-ex/9906043.
 - [50] NOMAD, A. Chukanov *et al.*, Eur. Phys. J. C **46**, 69 (2006), hep-ex/0604050.
 - [51] M. Anselmino, M. Bertini, F. Murgia, and P. Quintairos, Eur. Phys. J. C **2**, 539 (1998), hep-ph/9704420.
 - [52] M. Anselmino, M. Bertini, F. Murgia, and B. Pire, Phys. Lett. B **438**, 347 (1998), hep-ph/9805234.
 - [53] M. Anselmino, M. Bertini, F. Caruso, F. Murgia, and P. Quintairos, Eur. Phys. J. C **11**, 529 (1999), hep-ph/9904205.
 - [54] Q.-h. Xu, C.-x. Liu, and Z.-t. Liang, Phys. Rev. D **63**, 111301 (2001), hep-ph/0103267.
 - [55] Q.-h. Xu and Z.-t. Liang, Phys. Rev. D **67**, 114013 (2003), hep-ph/0304125.
 - [56] K.-b. Chen, W.-h. Yang, S.-y. Wei, and Z.-t. Liang, Phys. Rev. D **94**, 034003 (2016), 1605.07790.
 - [57] K.-b. Chen, W.-h. Yang, Y.-j. Zhou, and Z.-t. Liang, Phys. Rev. D **95**, 034009 (2017), 1609.07001.
 - [58] K.-b. Chen, Z.-t. Liang, Y.-k. Song, and S.-y. Wei, Phys. Rev. D **102**, 034001 (2020), 2002.09890.
 - [59] A. Bacchetta and P. J. Mulders, Phys. Rev. D **62**, 114004 (2000), hep-ph/0007120.
 - [60] M. Jacob and G. C. Wick, Annals Phys. **7**, 404 (1959).
 - [61] S. U. Chung, (1971).
 - [62] A. Lesnik *et al.*, Phys. Rev. Lett. **35**, 770 (1975).
 - [63] G. Bunce *et al.*, Phys. Rev. Lett. **36**, 1113 (1976).

- [64] J. Bensinger *et al.*, Phys. Rev. Lett. **50**, 313 (1983).
- [65] S. A. Gounlay *et al.*, Phys. Rev. Lett. **56**, 2244 (1986).
- [66] TASSO, M. Althoff *et al.*, Z. Phys. C **27**, 27 (1985).
- [67] ALEPH, D. Buskulic *et al.*, Phys. Lett. B **374**, 319 (1996).
- [68] OPAL, K. Ackerstaff *et al.*, Eur. Phys. J. C **2**, 49 (1998), hep-ex/9708027.
- [69] ALICE, S. Acharya *et al.*, Phys. Rev. Lett. **125**, 012301 (2020), 1910.14408.
- [70] X.-L. Sheng, S. Pu, and Q. Wang, Phys. Rev. C **108**, 054902 (2023), 2308.14038.
- [71] X.-L. Xia, H. Li, X.-G. Huang, and H. Zhong Huang, Phys. Lett. B **817**, 136325 (2021), 2010.01474.
- [72] J.-H. Gao, Phys. Rev. D **104**, 076016 (2021), 2105.08293.
- [73] F. Li and S. Y. F. Liu, (2022), 2206.11890.
- [74] D. Wagner, N. Weickgenannt, and E. Speranza, Phys. Rev. Res. **5**, 013187 (2023), 2207.01111.
- [75] W.-B. Dong, Y.-L. Yin, X.-L. Sheng, S.-Z. Yang, and Q. Wang, Phys. Rev. D **109**, 056025 (2024), 2311.18400.
- [76] B. Müller and D.-L. Yang, Phys. Rev. D **105**, L011901 (2022), 2110.15630, [Erratum: Phys.Rev.D 106, 039904 (2022)].
- [77] A. Kumar, B. Müller, and D.-L. Yang, Phys. Rev. D **108**, 016020 (2023), 2304.04181.
- [78] A. Manohar and H. Georgi, Nucl. Phys. B **234**, 189 (1984).
- [79] X.-L. Sheng, Q. Wang, and X.-N. Wang, Phys. Rev. D **102**, 056013 (2020), 2007.05106.
- [80] Z.-t. Liang, Off diagonal elements of the spin density matrix of vector mesons in heavy ion collisions, in *The 7th International Conference on Chirality, Vorticity and magnetic field in heavy ion collisions, July 2023, Beijing, China*, 2023, <https://indico.ihep.ac.cn/event/16043/>.
- [81] J.-p. Lv, Z.-h. Yu, Z.-t. Liang, Q. Wang, and X.-N. Wang, Phys. Rev. D **109**, 114003 (2024), 2402.13721.
- [82] Z. Zhang, J.-p. Lv, Z.-h. Yu, and Z.-t. Liang, (2024), 2406.03840.
- [83] D. Zubarev, V. Morozov, and G. Röpke, *Statistical Mechanics of Nonequilibrium Processes, Basic Concepts, Kinetic Theory* Statistical Mechanics of Nonequilibrium Processes (Wiley, 1996).
- [84] D. Zubarev, V. Morozov, and G. Röpke, *Statistical Mechanics of Nonequilibrium Processes, Statistical Mechanics of Nonequilibrium Processes. Volume 2: Relaxation and Hydrodynamic Processes* Statistical Mechanics of Nonequilibrium Processes (Wiley, 1997).
- [85] D. N. Zubarev, A. V. Prozorkevich, and S. A. Smolyanskii, Theoretical and Mathematical Physics **40**, 821 (1979).
- [86] J. I. Kapusta and C. Gale, *Finite-temperature field theory: Principles and applications* Cambridge Monographs on Mathematical Physics (Cambridge University Press, 2011).
- [87] K.-c. Chou, Z.-b. Su, B.-l. Hao, and L. Yu, Phys. Rept. **118**, 1 (1985).
- [88] J.-P. Blaizot and E. Iancu, Phys. Rept. **359**, 355 (2002), hep-ph/0101103.
- [89] Q. Wang, K. Redlich, H. Stoecker, and W. Greiner, Phys. Rev. Lett. **88**, 132303 (2002), nucl-th/0111040.
- [90] J. Berges, AIP Conf. Proc. **739**, 3 (2004), hep-ph/0409233.
- [91] W. Cassing, Eur. Phys. J. ST **168**, 3 (2009), 0808.0715.
- [92] M. Crossley, P. Glorioso, and H. Liu, JHEP **09**, 095 (2017), 1511.03646.
- [93] J. I. Kapusta and C. Gale, *Finite-Temperature Field Theory* Cambridge Monographs on Mathematical Physics (Cambridge University Press, 2023).
- [94] X.-L. Sheng, N. Weickgenannt, E. Speranza, D. H. Rischke, and Q. Wang, Phys. Rev. D **104**, 016029 (2021), 2103.10636.
- [95] Y. Hidaka, S. Pu, Q. Wang, and D.-L. Yang, Prog. Part. Nucl. Phys. **127**, 103989 (2022), 2201.07644.
- [96] X.-L. Sheng, Z.-T. Liang, and Q. Wang, Acta Phys. Sin. (in Chinese) **72**, 072502 (2023).
- [97] A. Fetter and J. Walecka, *Quantum Theory of Many-particle Systems* Dover Books on Physics (Dover Publications, 2003).
- [98] A. Hosoya, M.-a. Sakagami, and M. Takao, Annals Phys. **154**, 229 (1984).
- [99] F. Becattini, M. Buzzegoli, and E. Grossi, Particles **2**, 197 (2019), 1902.01089.
- [100] Y. L. Dokshitzer, Sov. Phys. JETP **46**, 641 (1977).
- [101] V. N. Gribov and L. N. Lipatov, Sov. J. Nucl. Phys. **15**, 438 (1972).
- [102] G. Altarelli and G. Parisi, Nucl. Phys. B **126**, 298 (1977).
- [103] J. F. Owens, Phys. Lett. B **76**, 85 (1978).
- [104] H. Georgi and H. D. Politzer, Nucl. Phys. B **136**, 445 (1978).
- [105] T. Uematsu, Phys. Lett. B **79**, 97 (1978).
- [106] V. Ravindran, Nucl. Phys. B **490**, 272 (1997), hep-ph/9607384.
- [107] V. Ravindran, Phys. Lett. B **398**, 169 (1997), hep-ph/9606273.